2
12-26-78

SAND78-8027
Unlimited Release

Joining by Plating: Optimization of Occluded Angle

J. W. Dini, H. R. Johnson, Y. R. Kan

Sandia Laboratories

SF 2900 Q(7-73)

MASTER

SAND78-8027
Unlimited Release
Printed November 1978

JOINING BY PLATING: OPTIMIZATION OF OCCLUDED ANGLE

J. W. Dini and H. R. Johnson
Materials Development Division I, 8312

Y. R. Kan
Applied Mechanics Division 8122
Sandia Laboratories, Livermore

ABSTRACT

An empirical method has been developed for predicting the minimum angle required for maximum joint strength for materials joined by plating. This is done through a proposed power law failure function, whose coefficients are taken from ring shear and conical head tensile data for plating/substrate combinations and whose exponent is determined from one set of plated-joint data. Experimental results are presented for Al-Ni-Al (7075-T6) and AM363-Ni-AM363 joints, and the failure function is used to predict joint strengths for Al-Ni-Al (2024-T6), UTi-Ni-UTi, and Be-Ti-Be.

CONTENTS

		Page
I.	Introduction	9
II.	Ring Shear and Tension Test Data for Nickel Plating	11
III.	Phenomenological Joint-Strength Function	15
IV.	Plated-Joint Data	20
V.	Comparison of Theory and Experiment	25
VI.	Conclusions	31
References		33

ILLUSTRATIONS

Figure		Page
1.	Steps in the Joining-by-Plating	10
2.	Ring Shear Test Specimen	12
3.	Conical Head Test Specimen	13
4.	Typical Plated Joint With Occluded Angle α Under an Axial Load σ	16
5.	Plots of the Failure Function $f(\sigma_n, \tau) = 0$ in the σ_n-τ Plane for Various Values of Exponent N	18
6.	Joint Strength σ as a Function of Occluded Angle α, Eq. (3), for Various Values of N	19
7.	Specifications for Tapered Joints	21
8.	Examples of Rods Joined by Plating	22
9.	Joint-Strength Data (Circles) as a Function of Occluded Angle for Al-Ni-Al (7075-T6)	23
10.	Joint-Strength Data (Circles) as a Function of Occluded Angle for AM363-Ni-AM363	24
11.	Fit of the Joint-Strength Function as a Function of Occluded Angle to the Al-Ni-Al (7075-T6) Data	26
12.	Comparison of the Joint-Strength Function for N = 1.2 (Solid Line) With Data for AM363-Ni-AM363	27
13.	Predicted Joint-Strength as a Function of Occluded Angle for Al-Ni-Al (2024-T6)	28
14.	Predicted Joint Strength as a Function of Occluded Angle for UTi-Ni-UTi	29

Figure (continued) Page

15. Predicted Joint Strength as a Function of Occluded Angle for Be-Ni-Be 30

TABLES

Table

I. Bond Strengths for Various Materials Plated With Nickel 14

II. Predicted and Measured Optimum Occluded Angles 31

JOINING BY PLATING: OPTIMIZATION OF OCCLUDED ANGLE

I. Introduction

Electroplating is sometimes used to join metals that cannot be joined by conventional techniques.[1,2] The process typically includes the machining of a taper on the parts to be joined, mating them, and building up the tapered region with thick electrodeposit, and then machining to final dimensions. Figure 1 shows the joining process pictorially. Complete details on the technique including applications and property data have already been reported.[1,2] The influence of the taper angle on the mechanical performance of the joint has not been rigorously addressed. Rather, design criteria, intuition, and experience have been used as guides to aid those wanting to use the process. The purpose of this work is to provide a method for analyzing the influence of the degree of taper on joint strength so that one can predict the minimum angle needed for optimum adhesion without having to fabricate and test a large number of joints.

In section II we present the results of shear and tension tests for nickel plating, the most commonly used electrodeposit for joining applications. The bond strengths obtained provide the primary input to the calculations. In section III a failure function for plated joints is proposed. It gives the joint

strength as a function of occluded angle, and is in the form of a power law whose exponent N must (at least within the scope of the analysis in this paper) be determined from a fit to one set of plate-joint data. Nickel-plated-joint experiments are taken up in section IV. From the aluminum data a determination of N is made and used to predict joint strengths for other parent materials (section V). A comparison of the theoretical calculations is made with AM363 stainless-steel joint data. Conclusions are given in section VI.

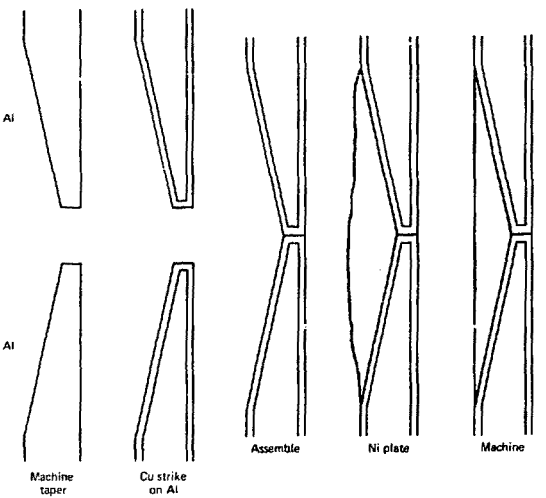

Figure 1. Steps in the Joining-by-Plating Process

II. Ring Shear and Tension Test Data for Nickel Plating

Quantitative shear and tensile strengths of plating-substrate combinations are more easily obtained than plated joint strength data. The techniques for obtaining these bond-strength data are basically as follows:

For the ring shear test, a cylindrical rod is coated with separate rings of electrodeposit of predetermined width. The rod is forced through a hole in a hardened steel die, the hole diameter being greater than that of the rod but less than that of the rod and the coating (Figure 2). The bond strength (interface shear strength) S_s (in MN/m^2 or psi) is determined by the formula $S_s = W/\pi dt$, where d is the diameter of the rod, t the width of the deposit, and W the force required to cause failure in the specimen.

For the tension test, samples are prepared by plating a flat substrate on both sides with thick electrodeposit. Conical-head specimens are machined from the composite and then tested with standard tension testing procedures. Figure 3 shows specimen dimensions and a cut-away view of a specimen under test. The normal tensile strength S_n is found from the formula $S_n = W/(\pi d^2/4)$.

Details for both of these tests are included in Reference 3 along with data and references for substrate-coating combinations tested by these techniques. Table I includes ring shear and conical-head tensile test data for a number of substrates of interest for potential joining by nickel plating applications. Included are values for 7075-T6 aluminum and AM363 stainless steel.

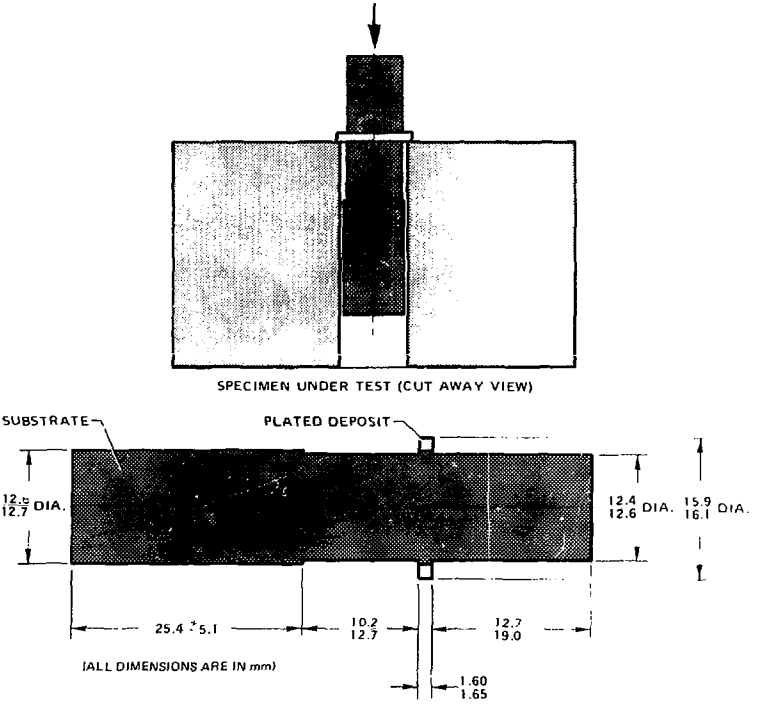

Figure 2. Ring Shear Test Specimen

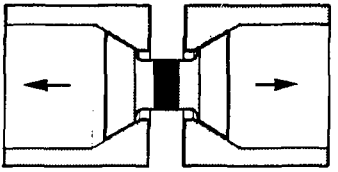

SPECIMEN UNDER TEST (CUT AWAY VIEW)

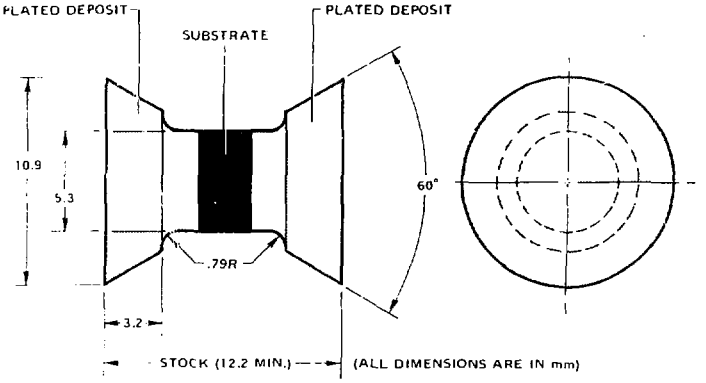

Figure 3. Conical Head Test Specimen

A comparison of the shear to tensile ratios for these two materials shows a wide variation, from 0.44 for aluminum compared to 0.94 for the AM363. These data were used to compute theoretical joint strengths as discussed in the following section.

TABLE I

BOND STRENGTHS FOR VARIOUS MATERIALS PLATED WITH NICKEL[a]

Material	Conical Head Tensile Strength (MN/m^2)	Conical Head Tensile Strength (psi)	Ring Shear Strength (MN/m^2)	Ring Shear Strength (psi)	Shear/Tensile Ratio
Beryllium	317	46,000	252	36,500	0.79
Uranium-0.8 Titanium	507	73,500	247	35,800	0.49
Aluminum (7075-T6)	572	83,000	250	36,200	0.44
Aluminum (2024-T6)	445	64,500	221	32,000	0.50
Stainless Steel (AM363)	490	71,000	455	60,000	0.94

[a]See reference 3 for details of these tests. Plating was done in a nickel sulfamate solution.

III. Phenomenological Joint-Strength Function

The objective of this analysis is to determine the minimum occluded angle α for optimum joint strength using the interface shear strength S_s and tensile strength S_n obtained experimentally from the ring shear and tension tests, respectively. However, as it will turn out, because of our lack of knowledge of how S_s and S_n interact to comprise the joint strength, it is also necessary to have some representative joint data for one parent material. The method of approach will be first to establish a failure criterion for the bonding interface. This will be used to find the joint strength as a function of S_s, S_n, α, and a parameter N which contains information on the coupling between S_s and S_n. A fit of the failure function to one set of joint data will then determine the value of N for that plating material, and thus α_{min} can be predicted for other parent materials with the same plating material.

When a joint is loaded axially, the bonded interface is under combined shear and tensile stresses. Figure 4 shows a sketch of a typical plated joint, with an occluded angle α, subjected to a nominal axial load σ applied at both ends. The detailed elastic stress field in the joint is very complex, and is a strong function of α and the parent and plated material properties. At the failure load, however, the stress state at the bonding interface is uniform because of the plasticity effect. The tensile stress σ_n and shear stress τ in the interface can be calculated from the equilibrium condition by the formulas

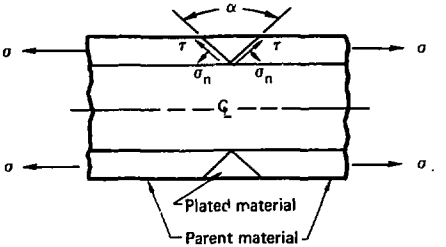

Figure 4. Typical Plated Joint With Occluded Angle α Under an Axial Load σ. τ and σ_n are the tensile and shear stresses, respectively.

$$\sigma_n = \frac{1}{2}\sigma\,(1 + \cos\alpha)\,, \qquad \tau = \frac{1}{2}\sigma \sin\alpha. \tag{1}$$

The proposed interface failure function is based on ideas developed by Mises and by Tresca.[4] The form suggested by their work is

$$f(s_n, \tau) = \left[(\sigma_n/S_n)^N + (\tau/S_s)^N\right]^{1/N} - 1 \tag{2}$$

where S_n is the normal tensile strength obtained from the conical head tension test, S_s the shear strength obtained from the ring shear test, and N a dimensionless constant (which will need to be determined from joint strength data). The experimentally determined $S_n = W/(\pi d^2/4)$ and $S_s = W/\pi dt$ do not take stress concentration into account. However, this is justifiable since any stress concentration at the bonding interface must be smoothed by local plasticity at the failure load so that the shear and tensile stresses are in fact uniform.

The failure function $f(\sigma_n, \tau)$ will never be greater than zero, and the failure criterion is $f(\sigma_n, \tau) = 0$. For $N = 2$ and $S_s/S_n = 1/\sqrt{3}$, $f(\sigma_n, \tau)$ becomes Mises' maximum distortion energy yield criterion for an isotropic material, while for $N = 2$ and $S_s/S_n = 1/2$ it is Tresca's maximum shear stress yield criterion. Both Mises' and Tresca's criteria incorporate the fact that the first stress invariant (the hydrostatic component) has no effect on yielding of the isotropic material. In plated joints, however, the ratio of shear to tensile strength can vary from 0.44 for Al-Ni-Al to 0.94 for AM363-Ni-AM363; in addition, the hydrostatic stress component does affect the failure at the interface. Therefore, even though the proposed failure function has the same form as Mises' and Tresca's yield criteria, it cannot be assumed that $N = 2$ will work. The value of N will depend on the degree of interaction between the shear and tensile stresses.

Figure 5 shows the failure function $f(\sigma_n, \tau)$ for some specific values of N. $N = \infty$ corresponds to no interaction between the shear and tensile stresses so that the presence of shear stress will not reduce the tensile strength of the interface, and vice versa. When $N = 2$, the Mises or Tresca ellipse, there is mild interaction; when $N = 1$, there is very strong interaction. Because of the interaction, the shear stress component considerably reduces the tensile strength of the interface.

By substituting σ_n and τ of Eq. (1) into the failure function, the joint strength σ can be expressed in terms of the occluded angle α, interface tensile strength S_n, shear strength S_s, and N by the equation

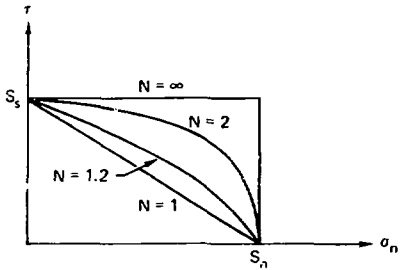

Figure 5. Plots of the Failure Function $f(\sigma_n, \tau) = 0$ in the $\sigma_n - \tau$ Plane for Various Values of Exponent N

$$\sigma = \left\{ \left(\frac{\frac{1}{2} + \frac{1}{2}\cos\alpha}{S_n} \right)^N + \left(\frac{\frac{1}{2}\sin\alpha}{S_s} \right)^N \right\}^{-\frac{1}{N}} . \tag{3}$$

The effect of power N on the joint strength σ at various occluded angles is plotted in Figure 6 for given interface tensile and shear strengths. The joint strength has a value of S_n at $\alpha = 0$ for all values of N when $S_n < S_p$, the strength of the parent material. For low N, σ first decreases with increasing α, reflecting the interaction between the shear and tensile stress components. The horizontal line $\sigma = S_p$ at larger values of α represents the tensile strength of the weakest material. Since joints can never be stronger than the tensile strength of the parent material, for large occluded angles the joint will fail in the parent material instead of the interface if angle α for $\sigma = S_p$ is the minimum occluded angle required to achieve the maximum joint strength. The value of N for joints with a given plating is determined from a fit of σ, as given in Figure 6, to a representative set of joint strength data.

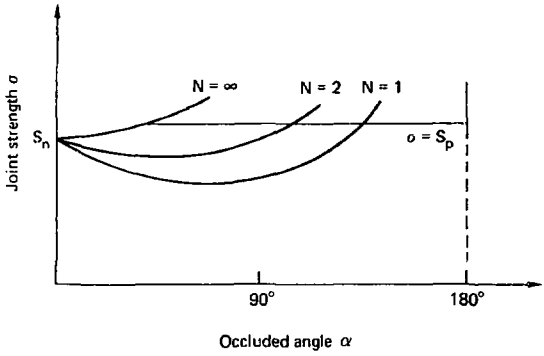

Figure 6. Joint Strength σ as a Function of Occluded Angle α, Eq. (3), for Various Values of N. The horizontal line $\sigma = S_p$ represents the strength of the parent material

IV. Plated-Joint Data

Since the widest variation in the ratio of shear to tensile strength in Table I is found for aluminum and stainless steel, it was decided to determine N from a fit to aluminum-nickel joint strength data and, based on that N value, to test the predicted values of joint strength against stainless steel data. One's confidence in the phenomenological theory for use with other parent materials would depend on the goodness of fit.

We joined aluminum rods (7075-T6) with nickel plating. The same was done with AM363 stainless-steel rods. On both sets of rods, tapers ranging from 4 to 55 degrees were used (Figure 7). All rods had an inner diameter of 3.2 mm (0.125 in.) and a wall thickness of 1.59 mm (0.0625 in.). For the joining process, an aluminum cylinder slightly less than 3.2 mm (0.125 in.) in diameter was inserted through the I. D. of the specimens to provide support and keep them aligned during nickel plating.

The zinc immersion method (zincating) was used for preparing aluminum for plating. This provides an adherent base onto which other metals can be deposited. For preparing stainless steel for plating, a Wood's nickel strike was used.[5] With this method, the oxide film is removed and replaced with a thin film of nickel, which serves as a base for subsequent plating.

After plating, the cylinders were removed and the outer diameters of the joined parts machined to final dimensions. Figure 8 shows some rods

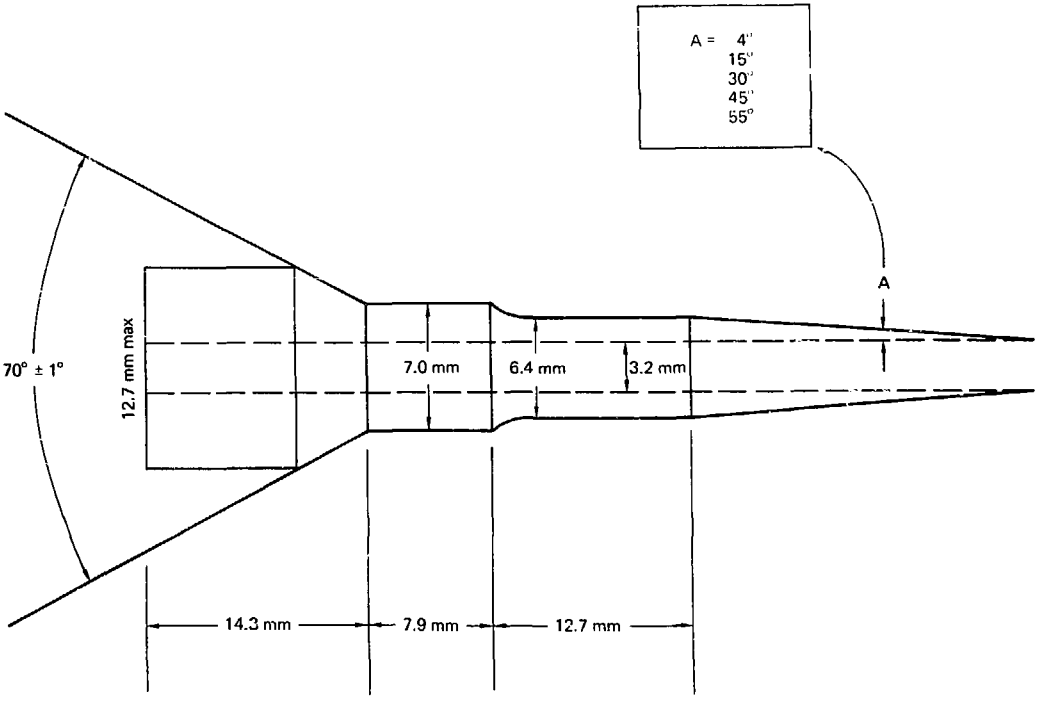

Figure 7. Specifications for Tapered Joints

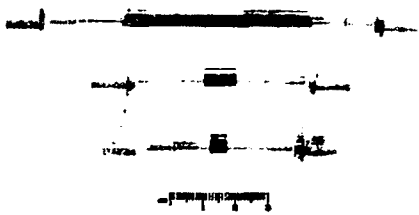

Figure 8. Examples of Rods Joined by Plating.
Shown are tube specimens with a 4° taper (top), 15° taper (middle), and 30° taper (bottom).

after joining. The rods were tested to failure by using an Instron machine and specially designed jaws.

The data for aluminum rods joined by nickel plating are presented in Figure 9. They show that maximum strength joints were obtained whenever the occluded angle was 120 degrees or greater. For angles less than 120 degrees, joint strengths progressively decreased as the occluded angle decreased. For occluded angles of 120 degrees or greater, failure always occurred in the aluminum. When the occluded angle was less than 120 degrees, failure occurred at the interface between the aluminum and the plating.

The data for the AM363 stainless-steel rods joined by nickel plating are presented in Figure 10. Maximum strength joints were obtained when the occluded angle was 90 degrees or greater.

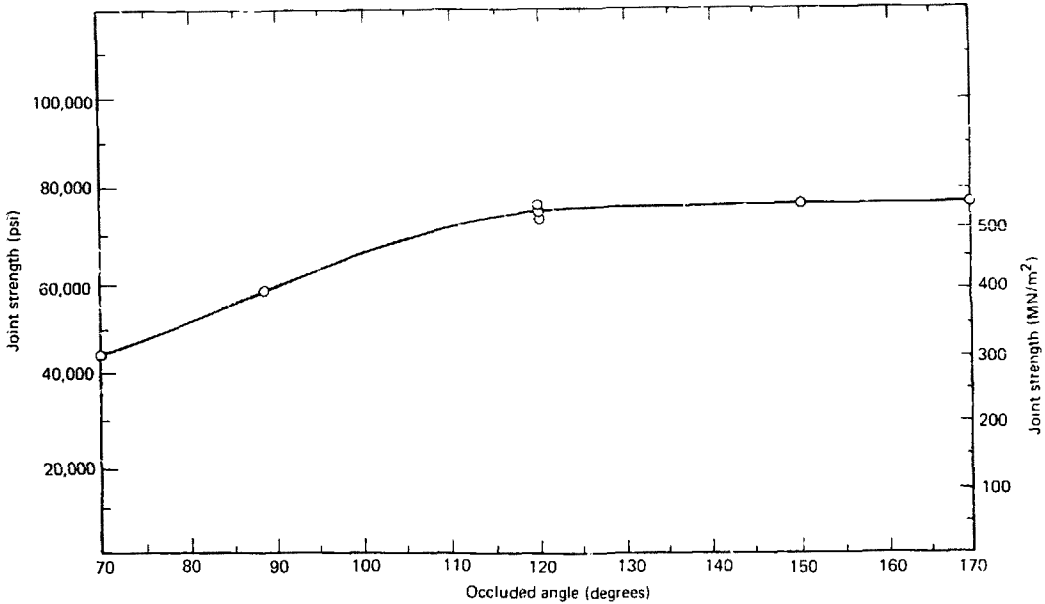

Figure 9. Joint-Strength Data (Circles) as a Function of Occluded Angle for Al-Ni-Al (7075-T6).
The curve is a guide for the eye only.

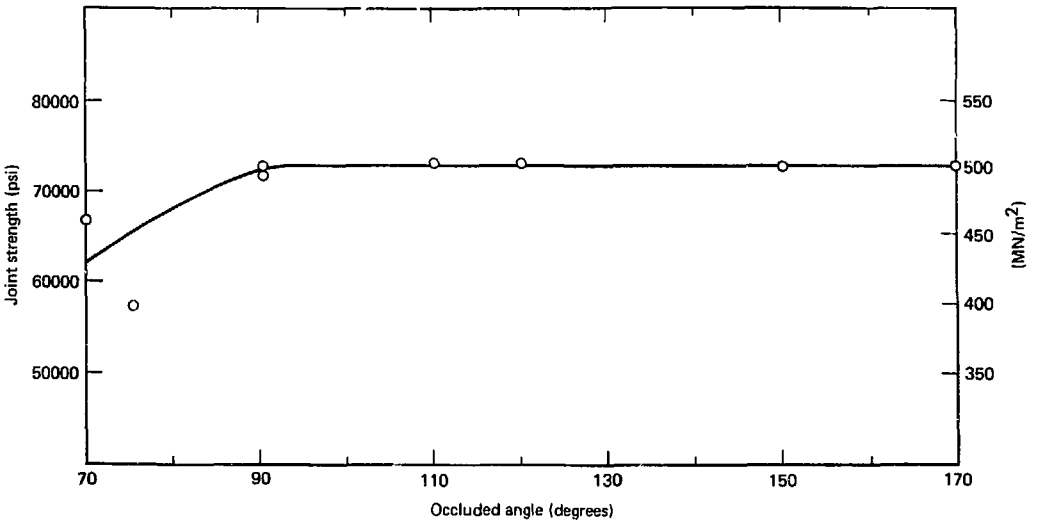

Figure 10. Joint-Strength Data (Circles) as a Function of Occluded Angle for AM363-Ni-AM363.
The curve is a guide for the eye only.

V. Comparison of Theory and Experiment

Figure 11 shows the measured Al-Ni-Al (7075-T6) joint data, represented by circles, and the failure function with N = 1, 1.2, 2, and ∞. The best fit is found for N = 1.2 (solid line). Corresponding data for AM363-Ni-AM363 are shown in Figure 12 along with the predicted curve for N = 1.2 (solid line) and, for comparison, curves for N = 1.0 and 2.0. The N = 1.2 fit is fairly good, although the N = 1.0 one is not unreasonable.

Using N = 1.2 for Al-Ni-Al (7075-T6) joint, the predicted optimum angle (the minimum angle for maximum joint strength, at $\sigma = S_p$) is 123 degrees, and the measured angle is about 120 degrees. The predicted optimum angle for AM363-Ni-AM363 joint is 83 degrees, and the measured angle is about 90 degrees. The weakest predicted joints for both aluminum alloy and stainless steel occur at $\alpha \simeq 70$ degrees. The reduction in strength for Al-Ni-Al (7075-T6) joint is about 159 MN/m^2 (from 524 MN/m^2 to 364 MN/m^2) and is about 48 MN/m^2 for AM363-Ni-AM363 joint (from 503 MN/m^2 to 455 MN/m^2). The large reduction in strength for the aluminum alloy joint is caused by its low ratio of interface shear strength to tensile strength (250 MN/m^2 to 572 MN/m^2).

Usint the shear and tensile strength data listed in Table I, the predicted joint strengths for Al-Ni-Al (2024-T6), Be-Ni-Be, and UTi-Ni-UTi joints are plotted in Figures 13 through 15. The predicted optimum angles are listed in

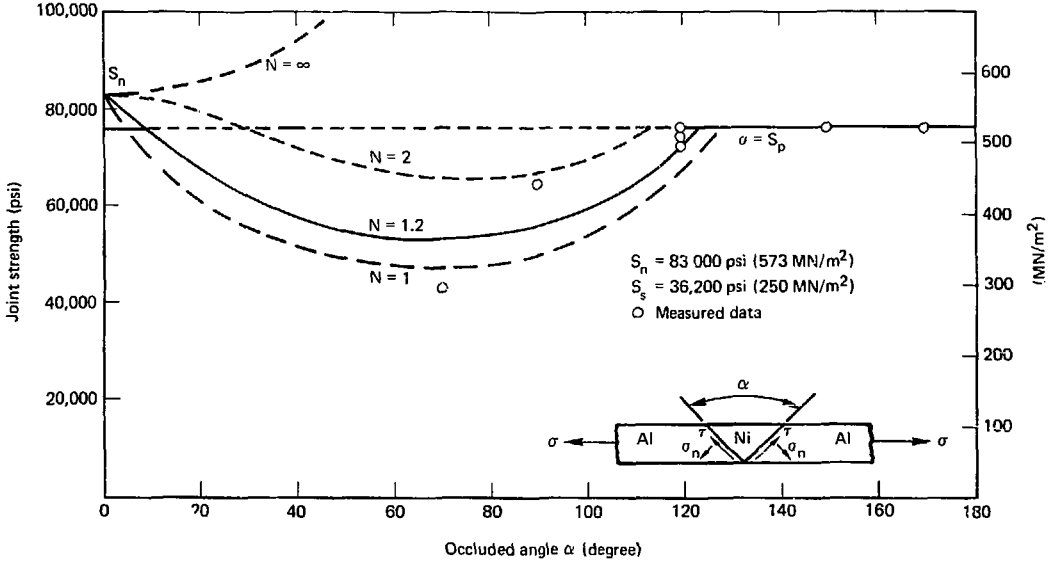

Figure 11. Fit of the Joint-Strength Function as a Function of Occluded Angle to the Al-Ni-Al (7075-T6) Data.
The N = 1.2 fit (solid line) is the best. Other fits (N = 1.0, 2.0, ∞) are shown as dashed curves.

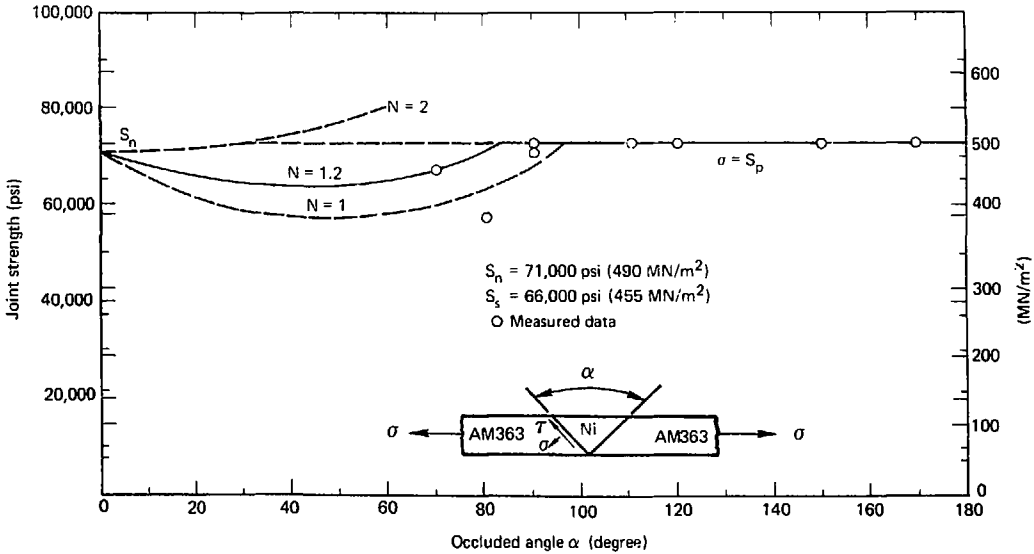

Figure 12. Comparison of the Joint-Strength Function for N = 1.2 (Solid Line) With Data for AM363-Ni-AM363. Also shown are theoretical curves (dashed) for N = 1.0 and 2.0.

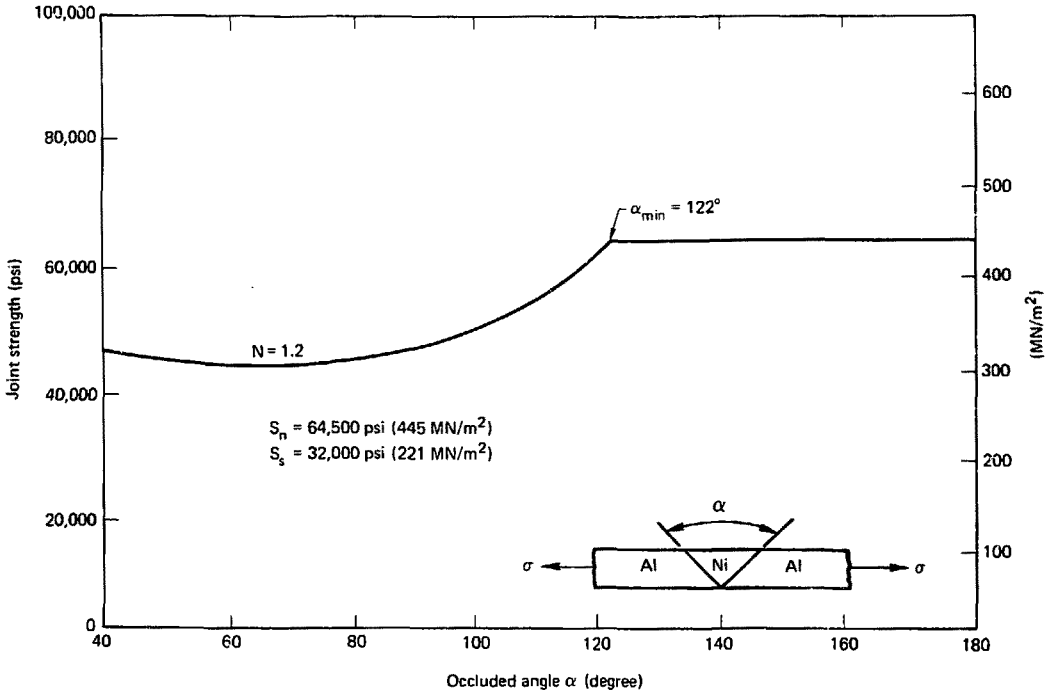

Figure 13. Predicted Joint Strength as a Function of Occluded Angle for Al-Ni-Al (2024-T6)

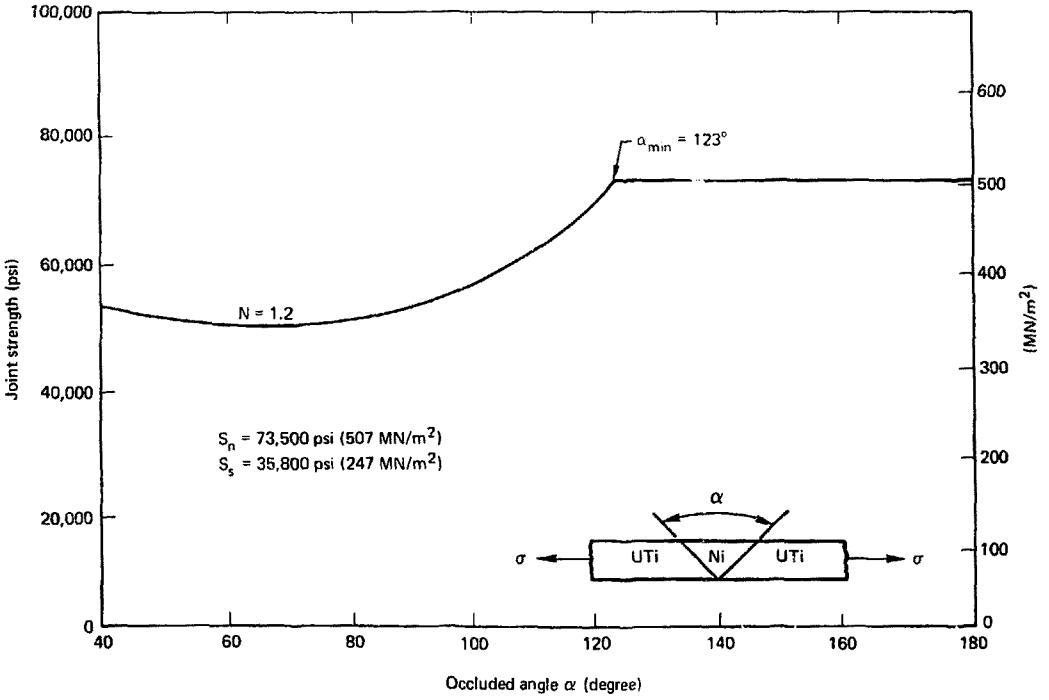

Figure 14. Predicted Joint Strength as a Function of Occluded Angle for UTi-Ni-UTi

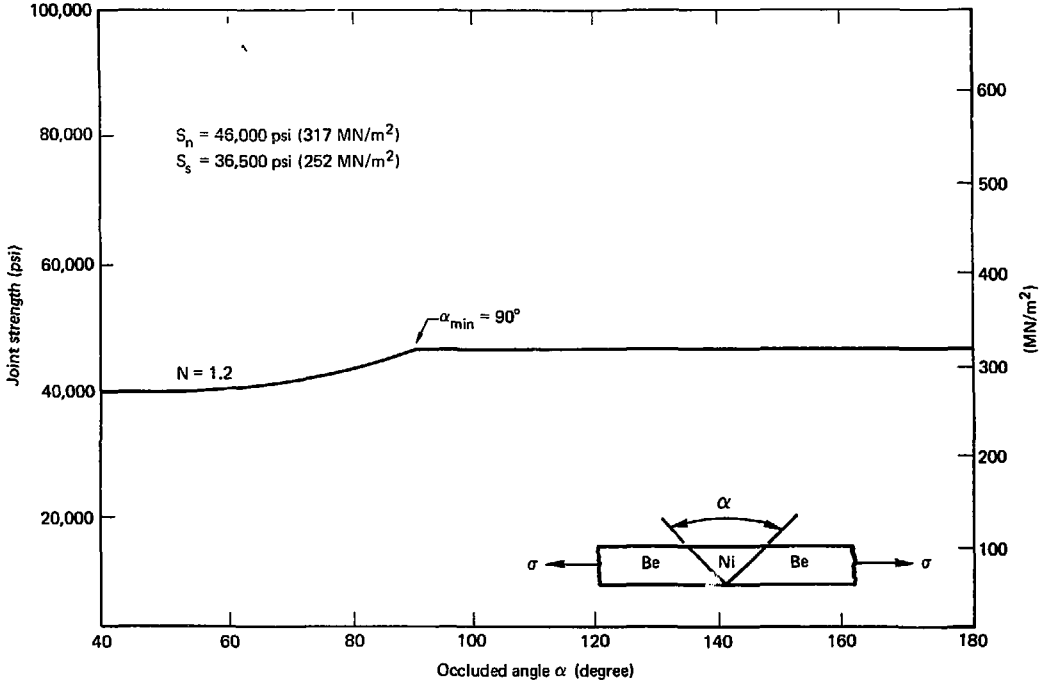

Figure 15. Predicted Joint Strength as a Function of Occluded Angle for Be-Ni-Be

Table II together with optimum angles for 7075-T6 aluminum alloy and AM363 stainless-steel joints. The very small predicted optimum angle (α = 90 degrees) for Be-Ni-Be is due to its high ratio of shear strength to tensile strength (=0.79).

TABLE II

PREDICTED AND MEASURED OPTIMUM OCCLUDED ANGLES

Material	Predicted Optimum Angle	Measured Optimum Angle
Al (7076-T6)	123°	120°
Stainless Steel (AM363)	83°	90°
Al (2024-T6)	122°	-
UTi	123°	-
Be	90°	-

VI. Conclusions

A failure criterion has been proposed for predicting the strength as a function of occluded angle of plated joints subjected to an axial load. It is in the form of a power law whose coefficients are extracted from shear and tension test data and whose exponent N must, for the present, be determined from a fit to a representative set of plated-joint data. For the case of nickel, data on Al-Ni-Al (7075-T6) showed N to be about 1.2, which was found to be consistent with AM363-Ni-AM363 data. The value of N of 1.2 appears to

represent a strong interaction between the shear and tensile stresses at the nickel-parent material interface.

We conclude that the proposed failure function can be used with confidence as a guide in fabricating nickel-plated joints with other materials. Predictions are given for the joint strengths as a function of occluded angle for Al-Ni-Al (2024-T6), UTi-Ni-UTi, and Be-Ni-Be. It would be of interest to test the failure function for other plating materials as well, to see if the general form is universal and, if so, to investigate the variation of N with plating material.

REFERENCES

1. J. W. Dini and H. R. Johnson, Metals Engineering Quarterly 14, No. 1, 6 (February 1974).
2. J. W. Dini and H. R. Johnson, "Electrochemical Joining: Process, Applications, and Property Data," SME Technical Paper AD75-855, Society of Manufacturing Engineers, Dearborn, Michigan, 1975.
3. J. W. Dini and H. R. Johnson, "Adhesion Testing of Deposit-Substrate Combinations," ASTM STP 640, 305 (1978).
4. R. Hill, "The Mathematical Theory of Plasticity," (Oxford Pres, 1967), pp. 15-23.
5. D. Wood, Metal Industry 36, 330 (1938).

UNLIMITED RELEASE

INITIAL DISTRIBUTION:

Bendix Corporation (6)
P. O. Box 1159
Kansas City, MO 64141
Attn: D. L. Stoltz

Union Carbide Corporation (3)
Y-12 Plant
P. O. Box Y
Oak Ridge, TN 37830
Attn: M. Bezik
F. B. Waldrop
R. Waldrop

Rockwell International (2)
Rocky Flats Plant
P.O. Box 464
Golden, CO 80401
Attn: G. Mah
R. Riegel
J. Krankota

W. K. Kelley, LLL, L-332
H. J. Wiesner, LLL, L-426
S. D. Holmes, 1473-3
R. S. Claassen, 5800
M. J. Davis, 5830
D. N. Mattox, 5834
T. B. Cook, Jr., 8000; Attn: A. N. Blackwell, 8200
L. Gutierrez, 8400
J. F. Barham, 8110
J. M. Stephenson, 8116
W. E. Alzheimer, 8120
C. S. Hoyle, 8122
Y. R. Kan, 8122 (10)
B. F. Murphey, 8300; Attn: T. S. Gold, 8320
J. L. Wirth, 8340
D. L. Hartley, 8350
D. M. Schuster, 8310
D. R. Adolphson, 8312
J. W. Dini, 8312 (10)
H. R. Johnson, 8312
R. W. Mar, 8313
W. R. Hoover, 8314
L. A. West, 8315
J. C. Swearengen, 8316

D. E. Gregson, 8440
R. C. Wayne, 8450
C. M. Tapp, 8460
Publications and Public Information Division, 8265, for TIC (2)
F. J. Cupps, 8265/Technical Library Processes Division, 3141
Technical Library Processes Division, 3141 (2)
Library and Security Classification Division, 8266-2 (3)